Published in final edited form as:
J Pharmacol Exp Ther. 2008 February ; 324(2): 475–483. doi:10.1124/jpet.107.131896.

Regression of Fibrosis after Chronic Stimulation of Cannabinoid CB2 Receptor in Cirrhotic Rats

Javier Muñoz-Luque, **Josefa Ros**, **Guillermo Fernández-Varo**, **Sònia Tugues**, **Manuel Morales-Ruiz**, **Carlos E. Alvarez**, **Scott L. Friedman**, **Vicente Arroyo**, and **Wladimiro Jiménez**
Biochemistry and Molecular Genetics Service (J.M.-L., J.R., G.F.-V., S.T., M.M.-R., W.J.), Department of Physiology I (W.J.) and Liver Unit (V.A.), Centro de Investigación Biomédica en Red de Enfermedades Hepaticas y Digestivas, Hospital Clínic, Institut d'Investigacions Biomèdiques August Pi i Sunyer, University of Barcelona, Barcelona, Spain; and Division of Liver Diseases, Mount Sinai School of Medicine, New York, New York (C.E.A., S.L.F.)

Abstract

Two cannabinoid (CB) receptor subtypes, CB1 and CB2, have been cloned and characterized. Among other activities, receptor activation by cannabinoid ligands may result in pro- or antifibrogenic effects depending on their interaction with CB1 or CB2, respectively. In the current study, we investigated whether selective activation of hepatic CB2 modifies collagen abundance in cirrhotic rats with ascites. mRNA and protein expression of CB receptors in the liver of control and cirrhotic rats was assessed by reverse transcription-polymerase chain reaction, Western blot, and immunohistochemistry. The effect of chronically activating the CB2 receptor was investigated in cirrhotic rats with ascites treated daily (9 days) with the CB2 receptor-selective agonist 3-(1,1-dimethylbutyl)-1-deoxy-Δ^8-tetrahydrocannabinol (JWH-133). At the end of treatment, mean arterial pressure and portal pressure were measured, and liver samples were obtained to evaluate infiltrate of mononuclear cells, hepatic apoptosis, α-smooth muscle actin (SMA) expression, collagen content, and matrix metalloproteinase (MMP)-2 abundance in all animals. JWH-133 improved arterial pressure, decreased the inflammatory infiltrate, reduced the number of activated stellate cells, increased apoptosis in nonparenchymal cells located in the margin of the septa, and decreased fibrosis compared with cirrhotic rats treated with vehicle. This was associated with decreased α-SMA and collagen I and increased MMP-2 in the hepatic tissue of cirrhotic rats treated with the CB2 agonist compared with untreated cirrhotic animals. Therefore, selective activation of hepatic CB2 receptors significantly reduces hepatic collagen content in rats with pre-existing cirrhosis, thus raising the possibility of using selective CB2 agonists for the treatment of hepatic fibrosis in human cirrhosis.

The discovery of specific membrane receptors of the marijuana component Δ^9-tetrahydrocannabinol in the early 1990s led to the identification of a novel endogenous signaling pathway, now known as the endocannabinoid system (Felder et al., 1992). This system is made up of the cannabinoid receptors, their endogenous ligands (or endocannabinoids), and the proteins for their synthesis and inactivation. The endogenous cannabinoid family includes anandamide (AEA), 2-arachydonyl glycerol, virodhamine, noladin ether, and *N*-arachidonoyl-dopamine. These substances promote their action through cannabinoid (CB) receptors. Two CB receptors, CB1 (Matsuda et al., 1990) and CB2 (Munro et al., 1993), have been cloned and characterized. Pharmacological evidence has suggested the presence of another as yet uncloned cannabinoid receptor (Begg et al., 2005). Moreover, AEA also interacts with the transient receptor potential (TRP) vanilloid type 1 protein, which is also

Address correspondence to: Dr. Wladimiro Jiménez, Servicio de Bioquímica y Genética Molecular, Hospital Clinic Universitari, Villarroel 170, Barcelona 08036, Spain. wjimenez@clinic.ub.es.

known as the VR1 receptor and belongs to the large family of TRP ion channels (Zygmunt et al., 1999). CB1 receptor is abundant in the brain, and it is involved in the control of motor activity, memory and cognition, emotion, sensory perception, and autonomic and endocrine functions. In addition, the CB1 receptor is expressed in peripheral nerve terminals and vascular endothelium. In contrast, CB2 receptors are expressed mainly by immune and hematopoietic cells, the modulation of cytokine release being one of their roles (Pacher et al., 2006).

Endocannabinoids may behave as pro- or antifibrogenic substances depending on their interaction with CB1 or CB2 receptors, respectively (Julien et al., 2005; Siegmund et al., 2005; Pacher et al., 2006). This raised the possibility that pharmacological modulation of the hepatic endocannabinoid system could be a valuable therapy in cirrhosis. In fact, activation of the CB1 receptor triggers fibrosis progression (Teixeira et al., 2006), whereas CB2 activation promotes antifibrogenic actions in the liver (Julien et al., 2005). In vitro and in vivo studies with CB2 knockout mice demonstrate that CB2 receptors inhibit the proliferation of hepatic stellate cells (HSC) and stimulate apoptosis through two different signaling routes involving induction of cyclooxygenase-2 and intracellular oxidative stress, respectively (Julien et al., 2005). In addition, selective blockade of CB1 receptors has been shown to inhibit fibrogenesis in mice (Teixeira et al., 2006). In the current study, we alternatively investigated whether selective long-term activation of hepatic CB2 receptors in rats with pre-existing cirrhosis and ascites decreases hepatic collagen abundance and therefore reverses fibrosis.

Materials and Methods

Induction of Cirrhosis in Rats

Studies were performed in male adult Wistar rats with cirrhosis, without or with ascites and in male adult Wistar control rats (Charles-River, Saint Aubin les Elseuf, France). Cirrhosis was induced by CCl_4 following a method described previously (Clària and Jiménez, 1999). Cirrhotic rats without ascites were studied between 11 and 12 weeks after starting the cirrhosis induction program. The absence of ascites was confirmed by laparotomy. Cirrhotic rats with ascites were studied between 13 and 17 weeks when ascites had fully developed. Control rats were studied after a similar period of phenobarbital administration. The study was performed according to the criteria of the Investigation and Ethics Committee of the Hospital Clínic Universitari.

CB1 and CB2 mRNA Expression in Hepatic Tissue

Total RNA was extracted from the middle liver lobe of control and cirrhotic rats and brain and spleen from control rats using a commercially available kit (TRIzol Reagent; Invitrogen, Carlsbad, CA). One microgram of total RNA was reverse transcribed (RT) by using a complementary DNA synthesis kit (Roche Applied Science, Indianapolis, IN). Primers for the CB1-receptor (sense, 5′-TGT-GGGCAGCCTGTTCCTCA-3′; antisense, 5′-GGGTTTTGGCCAG-CCTAATGTC-3′) and for the CB2-receptor (sense, 5′-TTCCCCCT-GATCCCCAACGACTAC-3′; antisense, 5′-CTCTCCACTCCGCAG-GGCATAAAT-3′), were prepared according to rat CB1 and CB2 mRNA sequences (GenBank accession numbers. NM_012784 and NM_020543, respectively). Primers were also synthesized to amplify the cDNA encoding HPRT, a constitutively expressed gene, as control. HPRT primers were designed as described previously (Tugues et al., 2005), giving rise to a 264-bp polymerase chain reaction (PCR) product from the cDNA base sequence of rat HPRT. PCR was performed for CB1, CB2, and HPRT using a DNA amplification kit (Invitrogen). The PCR products were sequenced to check correct amplification.

CB1 and CB2 Protein Expression in Hepatic Tissue of Control and Cirrhotic Rats

Samples were individually homogenized (PT 10-35 Polytron; Kinematica, Kriens-Luzern, Switzerland) in a 20 mM Tris-HCl, pH 7.4, containing 1% Triton X-100, 0.1% SDS, 50 mM NaCl, 2.5 mM EDTA, 1 mM $Na_4P_2O_7 \cdot 10H_2O$, 20 mM NaF, 1 mM Na_3VO_4, 2 mM Pefabloc (Roche Diagnostic, Mannheim, Germany), and a cocktail of protease inhibitors (Complete Mini; Roche Diagnostics, Basel, Switzerland). To detect the CB1 receptor, 80 μg of the denatured proteins was run on a 10% SDS-polyacrylamide gel, and then they were transferred to nitrocellulose membranes (Transblot transfer medium; Bio-Rad, Hercules, CA), which were blocked with 5% powdered nonfat milk in TTBS buffer (50 mM Tris-HCl, pH 8, containing 0.05% Tween 20 and 150 mM NaCl) overnight at 4°C. Next, they were incubated with a primary rabbit polyclonal antibody against the CB1 receptor (1:250; Cayman Chemical, Ann Arbor, MI), followed by incubation with horseradish peroxidase-conjugated anti-rabbit antibody (1:5000; GE Healthcare, Little Chalfont, Buckinghamshire, UK). To detect the CB2 receptor, 80 μg of the denatured proteins was run on a 10% SDS-polyacrylamide gel, and then they were transferred to nitrocellulose membranes, which were blocked with 5% powdered nonfat milk in TTBS buffer (50 mM Tris-HCl, pH 8, containing 0.05% Tween 20 and 150 mM NaCl) overnight at 4°C. Next, they were incubated with a primary rabbit polyclonal antibody against the CB2 receptor (1:750; Cayman Chemical), followed by incubation with horseradish peroxidase-conjugated anti-rabbit antibody (1:2000; GE Healthcare). Bands were visualized by chemiluminescence (ECL Western blotting analysis system; GE Healthcare). The relative expression of CB1 and CB2 receptors was determined by densitometric scanning.

Selective Activation of CB2 Receptors in Cirrhotic Rats with Ascites

Cirrhotic rats with ascites were included in the protocol after developing stable ascites. Thereafter, CCl_4 treatment was discontinued, and animals were randomly assigned to one of the following groups: group A, daily s.c. injection of the CB2 receptor-selective agonist JWH-133 (1 mg/kg b.wt.; Tocris Cookson, Inc., Bristol, UK; Huffman et al., 1999) for 9 days beginning the second week after the detection of sustained ascites; and group B, daily s.c. injection of saline solution (1 ml/kg b.wt.) containing 5% ethanol. At the end of the treatment, animals were anesthetized with inactin (50 mg $\cdot$ kg^{-1}) and mean arterial pressure (MAP) and portal pressure were recorded as described previously (Ros et al., 2005). Liver specimens were obtained from each animal, washed in 0.1% diethyl pyrocarbonate-treated phosphate-buffered saline salt solution (140 mM NaCl, 8.5 mM Na_2HPO_4, and 1.84 mM $Na_2HPO_4 \cdot H_2O$, pH 7.4), immediately frozen in dry ice, and stored in liquid nitrogen to evaluate collagen type I and matrix metalloproteinase (MMP)-2 expression. Liver samples from treated and untreated animals were also fixed in 10% buffered formalin for further hematoxylin and eosin and immunostaining analysis.

Immunodetection of CB2, CD68, and *α*-SMA-Positive Cells

Liver sections from cirrhotic rats with ascites chronically receiving the CB2 agonist or vehicle underwent microwave antigen retrieval to unmask antigens hidden by cross-linkage occurring during tissue fixation. Endogenous peroxidase activity was blocked by hydrogen peroxide pretreatment for 10 min, and it was then further blockaded by incubation with 5% goat serum for 45 min. Sections were then stained with rabbit polyclonal anti-rat CB2 antibody (1:300; Cayman Chemical), mouse anti-rat CD68, a lysosomal protein present in activated macrophages (clone ED1, 1:150; Serotec, Kidlington, Oxford, UK), or with mouse anti-rat α-smooth muscle actin (SMA) (1:1200; Dako Denmark A/S, Glostrup, Denmark) and incubated overnight at 4°C or 1.5 and 1 h, respectively, at room temperature. The LSAB 2 System-HRP (Dako Denmark A/S) was used for antigen detection, and antigen visualization was achieved with streptavidin peroxidase and counterstained with hematoxylin. Macrophages (CD68-positive cells) in the middle and margin of the septa were assessed by counting 16 random

fields (magnification 1000×) per each section. The mean cell count for each sample was calculated. The area of α-SMA-positive staining was visualized using a digital microscope (Eclypse E-600; Nikon, Kawasaki, Japan). Images were processed using a morphometric analysis system (AnalySIS, version 3.2 Soft Imaging System; Olympus, Tokyo, Japan). The percentage of immunostained/fields areas of digital photomicrographs was then quantified. As negative controls, immunostaining was performed without the first antibody.

Apoptosis in Hepatic Tissue

We used the terminal deoxynucleotidyl transferase dUTP nick-end labeling (TUNEL) assay to detect cell death using the fluorescein-FragEL DNA fragmentation detection kit (Calbiochem, San Diego, CA) according to the manufacturer's protocol. To quantify and compare the rates of cell death between groups, a semiquantitative scoring method was used. For each sample, the number of TUNEL-positive cells was counted per 200× high-power field. At least eight representative fields were evaluated for each treatment group, from which an average value was calculated.

Fibrosis Quantification

Liver sections (4 μm) were stained in 0.1% Sirius red F3B (Sigma-Aldrich, St. Louis, MO) in saturated picric acid (Sigma-Aldrich). Relative fibrosis area (expressed as a percentage of total liver area) was assessed by analyzing 36 fields of Sirius red-stained liver sections per animal. Each field was acquired at 10× magnification [E600 microscope (Nikon) and RT-Slider SPOT digital camera (Diagnostic Instruments, Inc., Sterling Heights, MI)], and then it was analyzed using a computerized Bioquant Life Science morphometry system. To evaluate the relative fibrosis area, the measured collagen area was divided by the net field area and then multiplied by 100. Subtraction of vascular luminal area from the total field area yielded the final calculation of the net fibrosis area. From each animal analyzed, the amount of fibrosis as percentage was measured and the average value presented.

Western Blot Analysis of Collagen Type I, MMP-2, α-SMA, and Activated Caspase-3

Hepatic tissue from treated and nontreated cirrhotic rats with ascites was individually homogenized as described previously. To detect collagen type I and MMP-2, 120 and 80 μg, respectively, of total denatured proteins were loaded on a 7.5% SDS-polyacrylamide gel. To detect α-SMA, 120 μg of total proteins was separated on a 10% SDS-polyacrylamide gel. To detect activated caspase-3, 80 μg of total proteins was separated on a 12% SDS-polyacrylamide gel (Mini Protean III; Bio-Rad). Gels for collagen type I and activated caspase-3 were transferred to nitrocellulose membranes for 2 h and blocked with 5% powdered nonfat milk in TTBS buffer overnight at 4°C. Gels for MMP-2, and α-SMA, were transferred overnight at 4° C to nitrocellulose membranes. All membranes were stained with Ponceau S Red as a control for protein loading, and then they were incubated at room temperature with mouse monoclonal anti-collagen type I (1:500 dilution; Abcam plc, Cambridge, UK), MMP-2 (1:750 dilution; Neomarkers, Fremont, CA), and α-SMA (1:250 dilution; Dako Denmark A/S) for 2 h or incubated at 4°C with rabbit polyclonal anti-activated caspase-3 (1:300 dilution; Abcam plc) for 48 h. The bands for collagen type I, MMP-2, α-SMA, and activated caspase-3 were visualized by chemiluminescence (ECL Western blotting analysis system; GE Healthcare).

Immunofluorescence

For immunofluorescence, tissues were fixed in 10% buffered formaldehyde solution and embedded in paraffin. Sections were underwent microwave antigen retrieval, blocked with 5% normal goat serum, and incubated with rabbit anti-active caspase-3, mouse anti-α-SMA, or mouse anti-CD68 antibodies. In addition, 4,6-diamidino-2-phenylindole (Vectashield; Vector laboratories, Burlingame, CA) was used to counterstain cell nuclei. Controls without primary

antibodies were used as negative controls. Binding sites of the primary antibodies were revealed with cyanine-3-conjugated goat anti-mouse IgG and with fluorescein isothiocyanate-conjugated goat-anti-rabbit IgG (Jackson ImmunoResearch Laboratories Inc., West Grove, PA). Samples were visualized with a fluorescence microscope (Eclipse E600).

Measurements and Statistical Analysis

Serum osmolality was determined from osmometric depression of the freezing point (Osmometer 3300; Advanced Instruments, Needham Heights, MA) and sodium concentration by flame photometry (IL 943; Instrumentation Laboratory, Lexington, MA). Serum albumin, alanine aminotransferase and lactate dehydrogenase were measured by the AD-VIA 1650 Instrument (Siemens Medical Solutions Diagnostics, Tarrytown, NY).

Statistical analysis of results was performed by unpaired Student's *t* tests when appropriate. Data are expressed as mean ± S.E.M., and they are considered significant at a p level of 0.05 or less.

Results

In total, the liver of the animals treated with CCl_4 included in the study had a finely granulated surface, and histological examination showed the characteristic features of cirrhosis. In those animals with ascites, the ascites volume ranged between 5 and 60 ml. Control rats displayed no appreciable alterations in the liver histology.

CB1 and CB2 mRNA Expression

DNA amplification products obtained from hepatic tissue of six cirrhotic and three control rats are shown in Fig. 1A. Total RNA was also obtained from brain and spleen of normal rats for positive controls of CB1 and CB2 receptors, respectively. Bands of 425, 369, and 264 bp corresponding to CB1 and CB2 receptors and HPRT mRNAs, respectively, were detected in all the samples analyzed, thus demonstrating expression of these transcripts in the liver tissue. Densitometric analysis of these results is shown in Fig. 1B. Both CB1 and CB2 transcript abundance was significantly higher in samples obtained from cirrhotic rats, regardless of whether they were obtained from animals without or with ascites. Therefore, gene expression of cannabinoid receptors was markedly activated in the cirrhotic liver.

CB1 and CB2 Protein Expression

Western blot analysis of CB1 receptor yielded a specific band at the expected molecular mass of ~53 kDa in the positive control. In contrast to the clear band found in the RT-PCR assays, no signal was detected in protein extracts isolated from hepatic tissue of both cirrhotic and control animals (Fig. 2). Because these findings were reproduced after using a different type of monoclonal anti-CB1 antibody (1:250; Chemicon International, Temecula, CA), these results probably reflect the relatively low abundance or dilution of this protein in whole hepatic tissue because the majority of cells (i.e., hepatocytes) did not express the receptor. Samples from liver of cirrhotic and control rats showed a specific band of ~51 kDa that was identified as CB2 protein, based on identical size as the positive control (Fig. 2A). Paralleling the increased CB2 mRNA, enhanced abundance of CB2 protein was detected in cirrhotic livers compared with controls. It is of interest that this increase in CB2 protein expression was mainly localized in portal tracts and fibrous septa (Fig. 2B).

Liver Function Tests, Mean Arterial Pressure, and Portal Pressure in Treated and Nontreated Cirrhotic Rats with Ascites

Table 1 shows biochemical tests of liver function and serum electrolytes in both groups of cirrhotic rats. No significant differences were observed in any of these parameters between treated and nontreated cirrhotic rats. Furthermore, cirrhotic rats receiving vehicle had significant hemodynamic dysfunction, as reflected by marked portal hypertension (13.9 ± 1.5 mm Hg) and arterial hypotension (80 ± 4 mm Hg). Administration of the CB2 receptor agonist to cirrhotic rats for 9 days resulted in a significant improvement in MAP (93 ± 2 mm Hg; $p < 0.05$) in the absence of any change in portal pressure (14.1 ± 1.0 mm Hg).

Effects of CB2 Receptor Activation on Infiltrating and Fibrogenic Cell Density and Apoptosis

Density of infiltrating monocytes/macrophages in the liver tissue of cirrhotic rats with ascites was assessed by determining the amount of CD68-positive cells within and at the margin of the portal tracts and septa. CD68 antigen was expressed in both JWH-133-treated and nontreated cirrhotic rats. The morphology of cells expressing CD68 in these regions of the liver sections predominantly occurred as round/oval-shaped cells (Fig. 3A), in accordance with infiltrating monocytes/macrophages. Of note was that the density of $CD68^+$ staining cells within and around the margins of the fibrous bands was significantly lower in the cirrhotic livers chronically treated with the CB2 receptor agonist compared with the cirrhotic livers receiving vehicle (Fig. 3B).

Activated HSC acquire a myofibroblastic phenotype that is characterized by expression of α-SMA, which is not detected in quiescent HSC. Thus, α-SMA is a well-validated marker of activated HSC (Schmitt-Gräff et al., 1991). We detected α-SMA as linear staining in the portal tracts and fibrous septa, which was intense in the severely fibrotic tissue of both groups of cirrhotic rats (Fig. 4A). However, staining was more diffuse in liver tissue of rats receiving JWH-133 than in the liver of vehicle-treated cirrhotic animals. As shown in Fig. 4B, the percentage of the liver tissue that stained for α-SMA was significantly reduced in rats after CB2 receptor agonist stimulation compared with paired untreated cirrhotic animals.

To explore whether any cell populations were driven to apoptosis by the CB2 agonist, we performed in situ detection of nuclear DNA fragmentation by the TUNEL assay in liver sections of treated and nontreated cirrhotic rats. As a positive control of the TUNEL assay, apoptosis was induced by incubation of liver sections with DNase I. No staining was observed in the negative control in which terminal deoxynucleotidyl transferase enzyme was omitted (data not shown). Liver sections from cirrhotic rats showed few positive TUNEL staining cells, with immunoreactivity localized to the margin of the fibrous septa (Fig. 5A). However, the number of positive cells for TUNEL staining significantly increased in hepatic sections of animals treated with JWH-133 compared with the vehicle group (8.4 ± 0.4 versus 6.4 ± 0.3 positive cells/field, respectively; $p < 0.05$). In addition, we measured the amount of active caspase-3 in livers of vehicle- or JWH-133-treated animals. As shown in Fig. 5B, the amount of activated caspase-3 was significantly higher in cirrhotic rats treated with JWH-133 than in the vehicle group. It is of interest that activated caspase-3 immunostaining colocalized with α-SMA and CD68-positive cells (Fig. 6). These findings indicate that chronic in vivo stimulation of CB2 receptors selectively promotes apoptosis in myofibroblastic and monocytic cell types located in the margin of the fibrous septa.

Effect of CB2 Receptor Activation on Liver Fibrosis in Cirrhotic Rats with Ascites

Sirius red, a dye that selectively binds collagen proteins, was used to stain the collagen fibrils in the liver of CCl_4-treated rats (Jimenez et al., 1985). As shown in Fig. 7A, both groups of rats had abundant fibrosis showing a characteristic pattern of perivenular and periportal deposition of connecting tissue with development of portal-to-portal septa, ending blind in the

parenchyma, and marked architectural distortion resulting in micronodular cirrhosis. However, biopsies obtained from cirrhotic rats receiving JWH-133 displayed thinner septa and more preserved hepatic parenchyma than nontreated cirrhotic animals. This was confirmed by the morphometric analysis of all Sirius red-stained sections in which samples of rats after chronic CB2 receptor stimulation showed a significant reduction in the percentage of fibrosis area than sections of vehicle-treated cirrhotic rats (Fig. 7B).

Effect of CB2 Receptor Activation on Protein Expression of α-SMA, Collagen I, and MMP-2 in the Liver of Cirrhotic Rats

In brief, we examined the effect of JWH-133 on hepatic expression of α-SMA, as a marker of HSC activation; collagen I, a fibril-forming collagen that predominates in chronic liver disease; and MMP-2, a matrix metalloproteinase that degrades collagen and other matrix proteins. As shown in Fig. 8, α-SMA and collagen I levels were significantly reduced in cirrhotic rats chronically receiving the CB2 receptor agonist compared with nontreated cirrhotic animals. In contrast, cirrhotic rats receiving JWH-133 for 9 days, expressed significantly more MMP-2 protein compared with cirrhotic animals receiving vehicle.

Discussion

Achieving regression of fibrosis has been a major challenge in patients with advanced liver disease. Although it was initially thought that hepatic cirrhosis was an irreversible phenomenon, there are currently numerous experimental indications suggesting that regression of hepatic cirrhosis is a realistic endpoint of therapy. Indeed, several resident hepatic cell types can degrade cellular matrix through the enzymatic action of MMPs, particularly those possessing type I collagenase activity (Han et al., 2004; Iredale, 2004; Siller-López et al., 2004). Moreover, different degrees of fibrosis regression have been demonstrated in a wide array of liver diseases, including viral hepatitis (Dufour et al., 1997; Kweon et al., 2001, Dienstag et al., 2003), biliary obstruction (Hammel et al., 2001), and nonalcoholic steatohepatitis (Dixon et al., 2004).

Recent studies in patients with chronic hepatitis C have demonstrated that daily cannabis smoking is an independent predictor of fibrosis progression (Hézode et al., 2005) and that steatosis severity is closely related to cannabis use (Hézode at al., 2007). These effects seem to be mediated through the interaction with the CB1 receptor, because activation of this receptor induces fatty acid synthesis and contributes to diet-induced obesity in mice (Osei-Hyiaman et al., 2005). Altogether, these results suggest that CB1 receptor activation could mediate fibrogenesis, thereby establishing the rationale for CB1 receptor blockade as an antifibrogenic therapeutic strategy in liver disease. This has been further supported by the results of Teixeira-Clerc et al. (2006), demonstrating that CB1 receptor antagonism decreases wound healing response to acute liver injury and the progression of fibrosis in different experimental models of liver disease. In contrast, increased cardiac and hepatic content of endogenous cannabinoids has been reported in cirrhosis (Bátkai et al., 2007a). This is probably the consequence of the increased endotoxemia occurring in this condition (Guarner et al., 1993), because bacterial lipopolysaccharide has been shown to increase anandamide synthesis in macrophages and hepatocytes (Bátkai et al., 2004).

Conversely to what occurs with CB1 receptors, experimental models indicate that the CB2 receptor counteracts liver fibrogenesis and induces growth inhibition and apoptosis in both human hepatic myofibroblasts and in hepatic stellate cells. Moreover, genetically engineered mice lacking the CB2 receptor are more susceptible to CCl_4-induced fibrosis than wild-type mice (Julien et al., 2005). In principle, activation of CB2 receptors may be a superior antifibrogenic strategy to CB1 receptor blockade, because CB2 receptor expression in the central nervous system is very low, and activation of this receptor mainly mediates anti-

inflammatory effects with no psychotropic effects (Van Sickle et al., 2005). Although CB1 receptor blockade offers the additional advantage of improving systemic hemodynamics (Ros et al., 2002), major arguments against this strategy are that CB1 receptors are largely located in the central nervous system and that they mediate important functions related to appetite, locomotion, and behavior (Pacher et al., 2006). Furthermore, humans treated with high doses of a CB1 receptor antagonist may present adverse events, including nausea, dizziness, anxiety, diarrhea, and depression (Després et al., 2005).

The results of the present study demonstrate marked mRNA up-regulation of both CB1 and CB2 receptors in the livers of cirrhotic rats. This is supported by previous studies showing that whereas mRNA expression is very faint in normal liver, there is intense induction in human and rodent liver with different degrees of fibrosis (Bátkai et al., 2001; Julien et al., 2005; Teixeira et al., 2006; Mendez-Sanchez et al., 2007). However, this was not paralleled by similar results on analyzing protein abundance of CB1 receptors. In fact, we were unable to detect any signal in protein extracts isolated from hepatic tissue of cirrhotic and control animals. Although CB1 receptors have been detected in hepatocytes, and endothelial and stellate cells (Bátkai et al., 2001; Biswas et al., 2003; Teixeira et al., 2006), our results probably reflect the low density of hepatic CB1 receptors, which can only be revealed with the use of purified plasma membranes, but not with crude liver homogenates (Osei-Hyiaman et al., 2005). It is also possible that these antibodies lack enough specificity/sensitivity to detect CB1 receptors in the liver homogenates. In contrast, a clear relationship was observed between the severity of fibrosis and CB2 receptor protein expression, i.e., no expression in normal rats and intense signal in rats with cirrhosis and ascites. Therefore, our findings indicate that the availability of CB2 receptors in the cirrhotic liver is much higher than that of CB1 receptors.

Because antifibrotic cannabinoid-based therapeutic strategies should minimize psychotropic side effects, we administered the CB2 receptor agonist JWH-133 to cirrhotic rats with ascites. This is among the most selective receptor agonists currently available commercially (Huffman et al., 1999). The binding affinity (K_i) for the CB2 and CB1 receptors is 3.4 and 677 nM, respectively, and previous experiments have provided pharmacological, biochemical, and behavioral evidence that JWH-133 selectively activates CB2 receptor in vivo in mice (Sánchez et al., 2001). Administration of JWH-133 to cirrhotic rats with ascites significantly improved MAP, decreased the inflammatory infiltrate, reduced activated HSC, increased apoptosis in myofibroblastic and monocytic cell types located in the margin of the septa, and decreased fibrosis compared with cirrhotic rats receiving vehicle. These findings were associated with decreased abundance of α-SMA and collagen I and increased content of MMP-2 in the hepatic tissue of cirrhotic rats treated with the CB2 receptor agonist in comparison with nontreated cirrhotic animals. Therefore, these results indicate that selective chronic stimulation of the CB2 receptor is effective in regressing fibrosis in experimental decompensated cirrhosis.

Recent studies by our laboratory (Tugues et al., 2007) have shown that fibrosis progression is associated with an inflammatory process characterized by induction of adhesion molecules in endothelial cells adjacent to areas of local inflammatory infiltrate, which favors the attraction of circulating cells to the activated vasculature where they adhere to and migrate into the liver parenchyma. This pattern of endothelial activation after liver injury is quite similar to that observed after hepatic ischemia reperfusion. In this latter condition, CB2 receptor agonists protect against the hepatic insult by decreasing endothelial cell activation, inflammatory response, expression of adhesion molecules, inflammatory cytokines and recruitment, and adhesion and activation of inflammatory cells (Bátkai et al., 2007b; Rajesh et al., 2007). Therefore, the antifibrogenic effect of CB2 stimulation in the cirrhotic animals could also be likely related to the anti-inflammatory effect associated with CB2 receptor stimulation.

Although the mechanisms of its action are not fully clarified, JWH-133 could act mainly by direct action on hepatic mesenchymal, fibrogenic cells. This view is supported by Julien et al. (2005), showing that CB2 receptors are strongly expressed in nonparenchymal cells and biliary cells located within and at the edges of fibrotic septa. These authors also showed that the growth arrest and apoptotic effects of cannabinoid receptor ligands are selectively mediated by CB2 receptors in human hepatic myofibroblasts. However, the current investigation could not exclude the possibility that JWH-133 exerts its beneficial effect through mechanisms other than those mediated by CB2 receptors. Siegmund et al. (2005) recently reported that the endocannabinoid AEA is a killer of activated HSC in vitro, a phenomenon not dependent on CB1, CB2, or TRP vanilloid type 1 protein receptor activation. Rather, the authors suggested that AEA induces cellular necrosis through its interaction with the membrane cholesterol, resulting in reactive oxygen species formation, intracellular Ca^{2+} release, and cell death.

There are numerous experimental data indicating that by interacting with vascular CB1 receptors, endocannabinoids are involved in the pathogenesis of the circulatory dysfunction occurring in advanced liver disease (Bátkai et al., 2001, 2007a; Ros et al., 2002; Domenicali et al., 2005). It is possible that among the most conclusive evidence is the fact that CB1 receptor blockade increases MAP in cirrhotic rats (Bátkai et al., 2001; Ros et al., 2002). Therefore, it is noteworthy that in the present investigation administration of the CB2 receptor agonist also improved blood pressure in cirrhotic animals. It has been demonstrated that endocannabinoid release directly correlates with hepatic damage and inflammation in ischemia/reperfusion injury (Bátkai et al., 2007b). Therefore, it is possible that in our study the CB2 agonist reduced endocannabinoid production by decreasing hepatic inflammation, thereby resulting in less endocannabinoid-mediated hypotension. This would be further supported by the fact that CB2 agonist administration did not produce significant hemodynamic effects in normal rodents (Bátkai et al., 2007b).

In summary, the results of the present investigation demonstrate that selective activation of hepatic CB2 receptors for 9 days significantly increases MAP, reduces the density of monocyte/macrophages within and around the margins of the portal tracts, decreases the amount of staining-positive α-SMA cells, increases apoptosis in myofibroblastic and in monocytic cell types, diminishes the tissue content of collagen I and α-SMA, and increases the abundance of the proteolytic enzyme MMP-2 in the liver of rats with pre-existing cirrhosis and ascites. These effects result in a significant reduction in the hepatic collagen content of cirrhotic animals, thus raising the possibility of using selective CB2 agonists for the treatment of hepatic fibrosis in advanced human liver disease, including cirrhosis.

Acknowledgments

This work was supported by Dirección General de Investigación Científica y Técnica Grants SAF03-02597 and SAF2006-07053 (to W.J.) and Grant SAF 07-63069 (to M.M.-R.). S.T. received a grant from Institut d'Investigacions Biomèdiques August Pi i Sunyer. J.M.-L. received Grant SAF03-02597 from Dirección General de Investigación Científica y Tecnológica. G.F.-V. received a Clinical Chemistry fellowship from Siemens Medical Solutions Diagnostics. S.L.F. was supported by National Institutes of Health Grant DK56621.

Abbreviations

AEA	anandamide
CB	cannabinoid
TRP	transient receptor potential
HSC	hepatic stellate cell(s)
HPRT	hypoxanthine-guanine phosphoribosyl transferase

bp	base pair(s)
RT	reverse transcription
PCR	polymerase chain reaction
JWH-133	3-(1,1-dimethylbutyl)-1-deoxy-Δ^8-tetrahydrocannabinol
MAP	mean arterial pressure
MMP	matrix metalloproteinase
SMA	smooth muscle actin
TUNEL	terminal deoxynucleotidyl transferase dUTP nick-end labeling

References

Bátkai S, Jarai Z, Wagner JA, Goparaju SK, Varga K, Liu J, Wang L, Mirshahi F, Khanolkar AD, Makriyannis A, et al. Endocannabinoids acting at vascular CB1 receptors mediate the vasodilated state in advanced liver cirrhosis. Nat Med 2001;7:827–832. [PubMed: 11433348]

Bátkai S, Mukhopadhyay P, Harvey-White J, Kechrid R, Pacher P, Kunos G. Endocannabinoids acting at CB1 receptors mediate the cardiac contractile dysfunction in cirrhotic rats. Am J Physiol Heart Circ Physiol 2007a;293:H1689–H1695.

Bátkai S, Osei-Hyiaman D, Pan H, El-Assal, Rajesh M, Mukhopadhyay P, Hong F, Harvey-White J, Jafri A, Hasko G, et al. Cannabinoid-2 receptor mediates protection against hepatic ischemia/reperfusion injury. FASEB J 2007b;21:1788–1800.

Bátkai S, Pacher P, Osei-Hyiaman D, Radaeva S, Liu J, Harvey-White J, Offertáler L, Rudd MA, Bukoski RF, Kunos G. Endocannabinoids acting at cannabioind-1 receptors regulate cardiovascular function in hypertension. Circulation 2004;110:1996–2002. [PubMed: 15451779]

Begg M, Pacher P, Batkai S, Osei-Hyiaman D, Offertaler L, Mo FM, Liu J, Kunos G. Evidence for novel cannabinoid receptors. Pharmacol Ther 2005;106:133–145. [PubMed: 15866316]

Biswas KK, Sarker KP, Abeyama K, Kawahara K, Iino S, Otsubo Y, Saigo K, Izumi H, Hashiguchi T, Yamakuchi M, et al. Membrane cholesterol but not putative receptors mediates anandamide-induced hepatocyte apoptosis. Hepatology 2003;38:1167–1177. [PubMed: 14578855]

Clària, J.; Jiménez, W. Renal dysfunction and ascites in Carbon-Tetrachloride-induced cirrhosis in rats. In: Arroyo, V.; Ginés, P.; Rodés, J.; Schrier, RW., editors. Ascites and Renal Dysfunction in Liver Disease Pathogenesis Diagnosis and Treatment. Blackwell Science Inc.; Malden, MA: 1999. p. 379-396.

Després JP, Golay A, Sjoström L. Effects of Rimonabant on metabolic risk factors in overweight patients with dyslipidemia. N Engl J Med 2005;353:2121–2134. [PubMed: 16291982]

Domenicali M, Ros J, Fernández-Varo G, Cejudo-Martín P, Crespo M, Morales-Ruiz M, Briones AM, Campistol JM, Arroyo V, Vila E, et al. Increased anandamide induced relaxation in mesenteric arteries of cirrhotic rats: role of cannabinoid and vanilloid receptors. Gut 2005;54:522–527. [PubMed: 15753538]

Dienstag JL, Goldin RD, Heathcote EJ, Hann HW, Woessner M, Stephenson SL, Gardner S, Gray DF, Schiff ER. Histological outcome during long-term lamivudine therapy. Gastroenterology 2003;124:105–117. [PubMed: 12512035]

Dixon JB, Bhathal PS, Hughes NR, O'Brien PE. Nonalcoholic fatty liver disease: improvement in liver histological analysis with weight loss. Hepatology 2004;39:1647–1654. [PubMed: 15185306]

Dufour JF, DeLellis R, Kaplan MM. Reversibility of hepatic fibrosis in autoimmune hepatitis. Ann Intern Med 1997;127:981–985. [PubMed: 9412303]

Felder CC, Veluz JS, Williams HL, Briley EM, Matsuda LA. Cannabinoid agonists stimulate both receptor- and non-receptor-mediated signal transduction pathways in cells transfected with and expressing cannabinoid receptor clones. Mol Pharmacol 1992;42:838–845. [PubMed: 1331766]

Guarner C, Soriano G, Tomas A, Bulbena O, Novella MT, Balanzo J, Vilardell, Murelle M, Moncada S. Increased serum nitrite and nitrate levels in patients with cirrhosis: relationship to endotoxemia. Hepatology 1993;18:1139–1143. [PubMed: 8225220]

Hammel P, Couvelard A, O'Toole D, Ratouis A, Sauvanet A, Flejou JF, Degott C, Belghiti J, Bernades P, Valla D, et al. Regression of liver fibrosis after biliary drainage in patients with chronic pancreatitis and stenosis of the common bile duct. N Engl J Med 2001;344:418–423. [PubMed: 11172178]

Han YP, Zhou L, Wang J, Xiong S, Garner WL, French SW, Tsukamoto H. Essential role of matrix metalloproteinases in interleukin-1-induced myofibroblastic activation of hepatic stellate cell in collagen. J Biol Chem 2004;279:4820–4828. [PubMed: 14617627]

Hézode C, Roudot-Thoraval F, Nguyen S, Grenard P, Julien B, Zafrani ES, Pawlostky JM, Dhumeaux D, Lotersztajn S, Mallat A. Daily cannabis smoking as a risk factor for progression of fibrosis in chronic hepatitis C. Hepatology 2005;42:63–71. [PubMed: 15892090]

Hézode C, Zafrani ES, Roudot-Thoraval F, Costentin C, Hessami A, Pawlotsky JM, Lotersztajn S, Mallat. A cannabis use as an independent predictor of severe steatosis during chronic hepatits C. J Hepatol 2007;46(Suppl 1):S10.

Huffman JW, Liddle J, Yu s, Aung MM, Abood ME, Wiley JL, Martin BR. 3-(1′,1′-Dimethylbutyl)-1-deoxy-Δ^8-THC and related compounds: synthesis of selective ligands for the CB2 receptors. Bioorg Med Chem 1999;7:2905–2914. [PubMed: 10658595]

Iredale JP. A cut above the rest? MMP-8 and liver fibrosis gene therapy. Gastroenterology 2004;126:1199–1201. [PubMed: 15057760]

Jimenez W, Pares A, Caballeria J, Heredia D, Bruguera M, Torres M, Rojkind M, Rodes J. Measurement of fibrosis in needle liver biopsies: evaluation of a colorimetric method. Hepatology 1985;5:815–818. [PubMed: 4029893]

Julien B, Grenard P, Teixeira-Clerc F, Van Nhieu JT, Li L, Karsak M, Zimmer A, Mallat A, Lotersztajn S. Antifibrogenic role of the cannabinoid receptor CB2 in the liver. Gastroenterology 2005;128:742–755. [PubMed: 15765409]

Kweon YO, Goodman ZD, Dienstag JL, Schiff ER, Brown NA, Burchardt E, Schoonhoven R, Brenner DA, Fried MW. Decreasing fibrogenesis: an immunohistochemical study of paired liver biopsies following lamivudine therapy for chronic hepatitis B. J Hepatol 2001;35:749–755. [PubMed: 11738102]

Matsuda LA, Lolait SJ, Brownstein MJ, Young AC, Bonner TI. Structure of a cannabinoid receptor and functional expression of the cloned cDNA. Nature 1990;346:561–564. [PubMed: 2165569]

Mendez-Sanchez N, Zamora-Valdes D, Pichardo-Bahena R, Barredo-Prieto B, Ponciano-Rodriguez G, Bermejo-Martinez L, Chavez-Tapia NC, Baptista-Gonzalez HA, Uribe M. Endocannabinoid receptor CB2 in nonalcoholic fatty liver disease. Liver Int 2007;27:215–219. [PubMed: 17311616]

Munro S, Thomas KL, Abu-Shaar M. Molecular characterization of a peripheral receptor for cannabinoids. Nature 1993;365:61–65. [PubMed: 7689702]

Osei-Hyiaman D, DePetrillo M, Pacher P, Liu J, Radaeva S, Batkai S, Harvey-White J, Mackie K, Offertaler L, Wang L, et al. Endocannabinoid activation at hepatic CB1 receptors stimulates fatty acid synthesis and contributes to diet-induced obesity. J Clin Invest 2005;115:1298–1305. [PubMed: 15864349]

Pacher P, Batkai S, Kunos G. The endocannabinoid system as an emerging target of pharmacotherapy. Pharmacol Rev 2006;58:389–462. [PubMed: 16968947]

Rajesh M, Pan H, Mukhopadhyay P, Batkai S, Osei-Hyiaman, Haskó G, Liaudet L, Gao B, Pacher P. Pivotal advance: cannabinoid-2 receptor agonist HU-308 protects against hepatic ischemia/reperfusion injury by attenuating oxidative stress, inflammatory response and apoptosis. J Leukoc Biol 2007;82:1382–1389. [PubMed: 17652447]

Ros J, Clària J, To-Figueras J, Planagumà A, Cejudo-Martín P, Fernández-Varo G, Martín-Ruiz R, Arroyo V, Rivera F, Rodés J, et al. Endogenous cannabinoids: a new system involved in the homeostasis of arterial pressure in experimental cirrhosis in the rat. Gastroenterology 2002;122:85–93. [PubMed: 11781284]

Ros J, Fernández-Varo G, Muñoz-Luque J, Arroyo V, Rodés J, Gunnet JW, Demarest KT, Jiménez W. Sustained aquaretic effect of the V2-AVP receptor antagonist, RWJ-351647, in cirrhotic rats with ascites and water retention. Br J Pharmacol 2005;146:654–661. [PubMed: 16113688]

Sánchez C, Ceballos ML, Gomez del Pulgar T, Rueda D, Corbacho C, Velasco G, Galve-Roperh I, Huffman JW, Ramón y Cajal S, Guzman M. Inhibition of glioma growth in vivo by selective activation of the CB2 cannabinoid receptor. Cancer Res 2001;61:5784–5789. [PubMed: 11479216]

Schmitt-Gräff A, Kruger S, Bochard F, Gabbiani G, Denk H. Modulation of alpha smooth muscle actin and desmin expression in perisinusoidal cells of normal and diseased human livers. Am J Pathol 1991;138:1233–1242. [PubMed: 2024709]

Siegmund SV, Uchinami H, Osawa Y, Brenner DA, Schwabe RF. Anandamide induces necrosis in primary hepatic stellate cells. Hepatology 2005;41:1085–1095. [PubMed: 15841466]

Siller-López F, Sandoval A, Salgado S, Salazar A, Bueno M, Garcia J, Vera J, Galvez J, Hernandez I, Ramos M, et al. Treatment with human metalloproteinase-8 gene delivery ameliorates experimental rat liver cirrhosis. Gastroenterology 2004;126:1122–1133. [PubMed: 15057751]

Teixeira-Clerc F, Julien B, Grenard P, Tran VN, Deveaux V, Li L, Serriere-Lanneau V, Ledent C, Mallat A, Lotersztajn S. CB1 cannabinoid receptor antagonism: a new strategy for the treatment of liver fibrosis. Nat Med 2006;12:671–676. [PubMed: 16715087]

Tugues S, Morales-Ruiz M, Fernandez-Varo G, Ros J, Arteta D, Muñoz-Luque J, Arroyo V, Rodes J, Jimenez W. Microarray analysis of endothelial differentially expressed genes in liver of cirrhotic rats. Gastroenterology 2005;129:1686–1695. [PubMed: 16285966]

Tugues S, Fernandez-Varo G, Muñoz-Luque J, Ros J, Arroyo V, Rodes J, Friedman SL, Carmeliet P, Jimenez W, Morales-Ruiz M. Antiangiogenic treatment with Sunitinib ameliorates inflammatory infiltrate, fibrosis and portal pressure in cirrhotic rats. Hepatology 2007;46:1919–1926. [PubMed: 17935226]

Van Sickle MD, Duncan M, Kingsley PJ, Moulhate A, Urbani P, Macckie K, Stella N, Makriyanis A, Piomelli D, Davison JS, et al. Identification and functional characterization of brainstem cannabinoid CB2 receptors. Science 2005;310:329–332. [PubMed: 16224028]

Zygmunt PM, Petersson J, Andersson DA, Chuang H, Sorgard M, Di M, Julius D, Hogestatt ED. Vanilloid receptors on sensory nerves mediate the vasodilator action of anandamide. Nature 1999;400:452–457. [PubMed: 10440374]

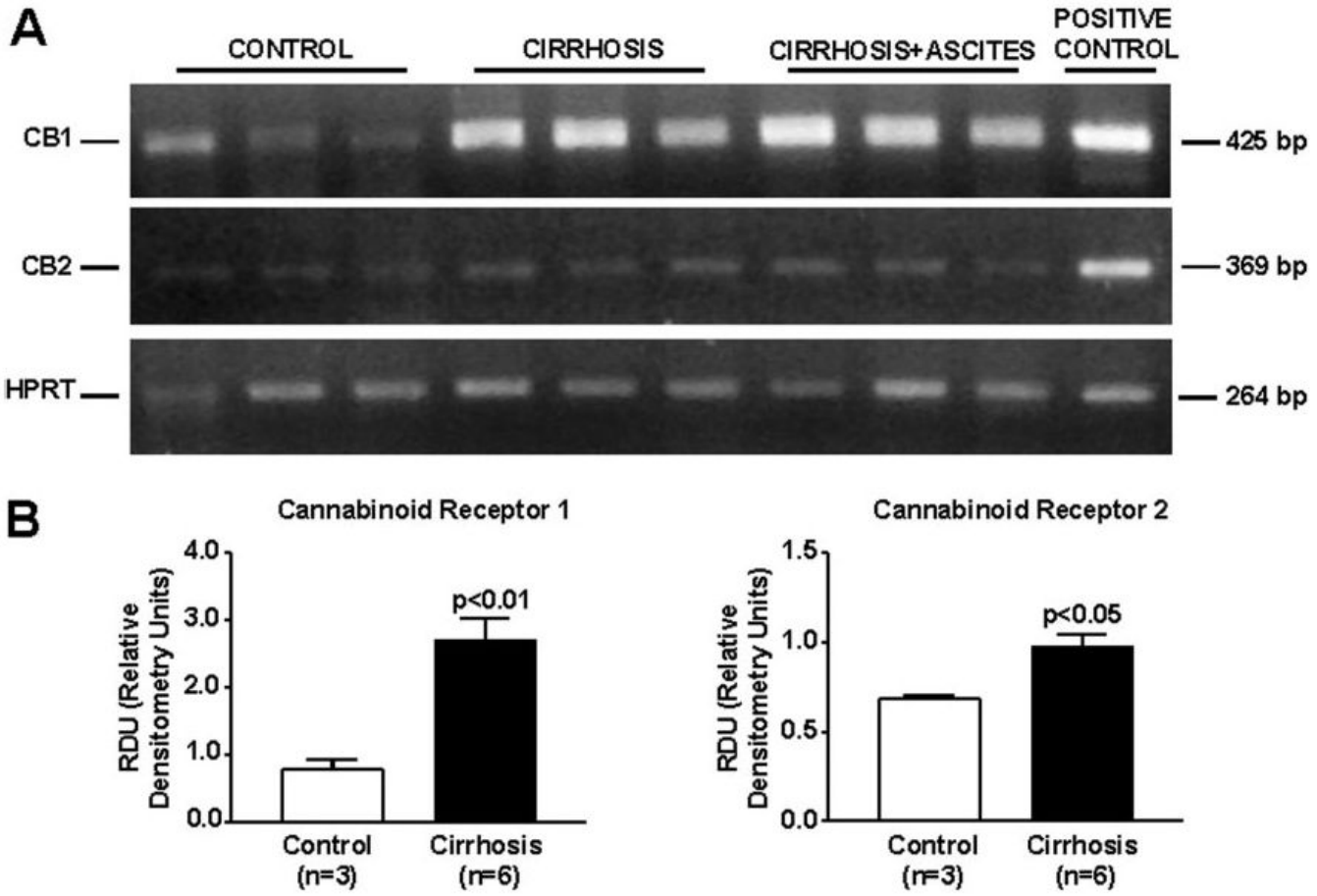

Fig. 1.

RNA expression of cannabinoid receptors in the liver of cirrhotic rats. Reverse transcription-polymerase chain reaction of mRNA for CB1 and CB2 receptors in hepatic tissue of three control and six cirrhotic rats. A, HPRT was amplified as a housekeeping gene. B, densitometric analysis of RT-PCR is shown at the bottom.

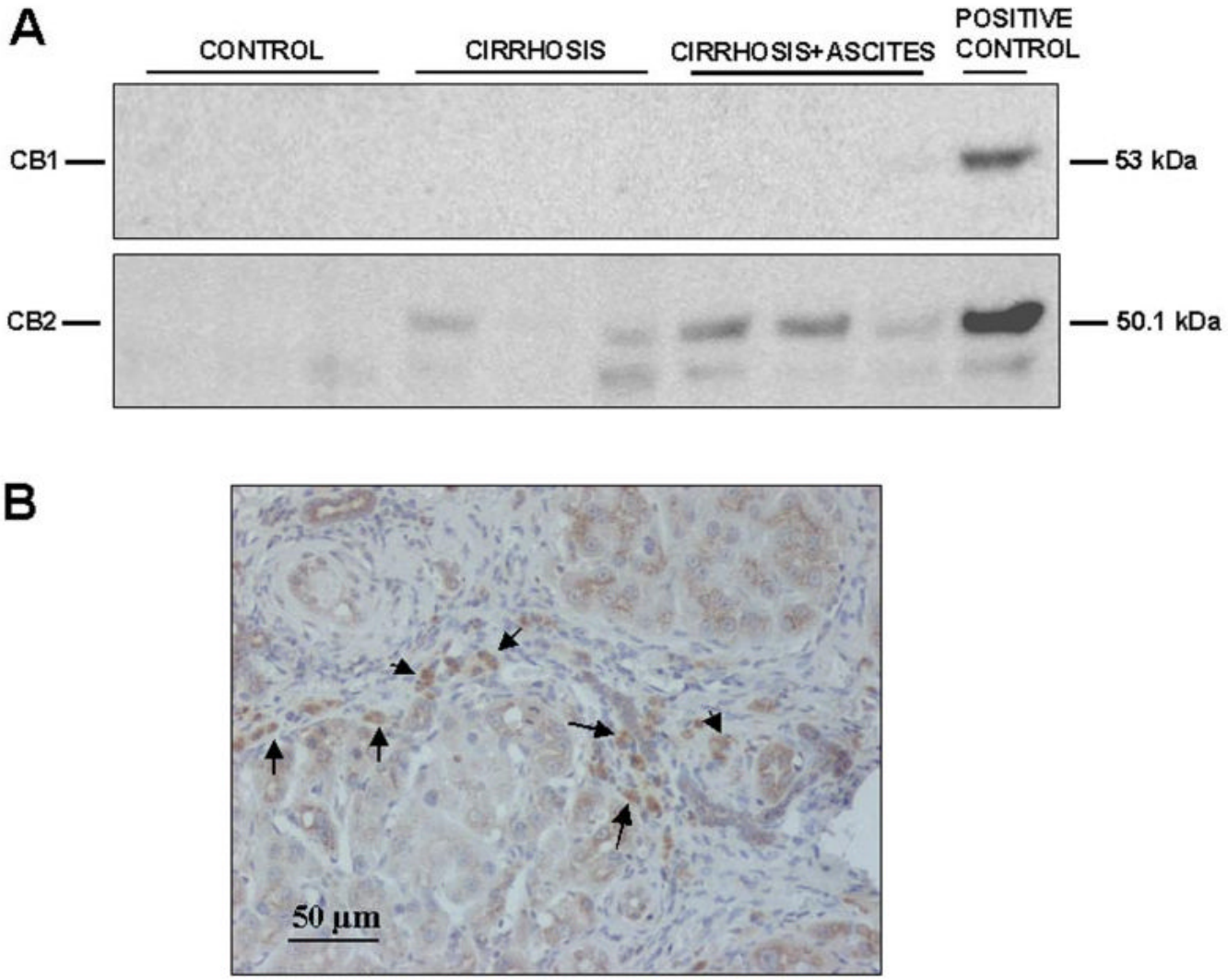

Fig. 2.

Protein expression of cannabinoid receptors in the liver of cirrhotic rat. A, Western blot for CB1 (top) and CB2 receptor (bottom) in liver tissue of three control rats and six cirrhotic rats. Eighty micrograms of protein extracts was loaded per lane. B, CB2-positive cells (arrows) was visualized in cirrhotic rats by immunostaining of paraffin liver sections with anti-CB2 antibody (original magnification, 200×).

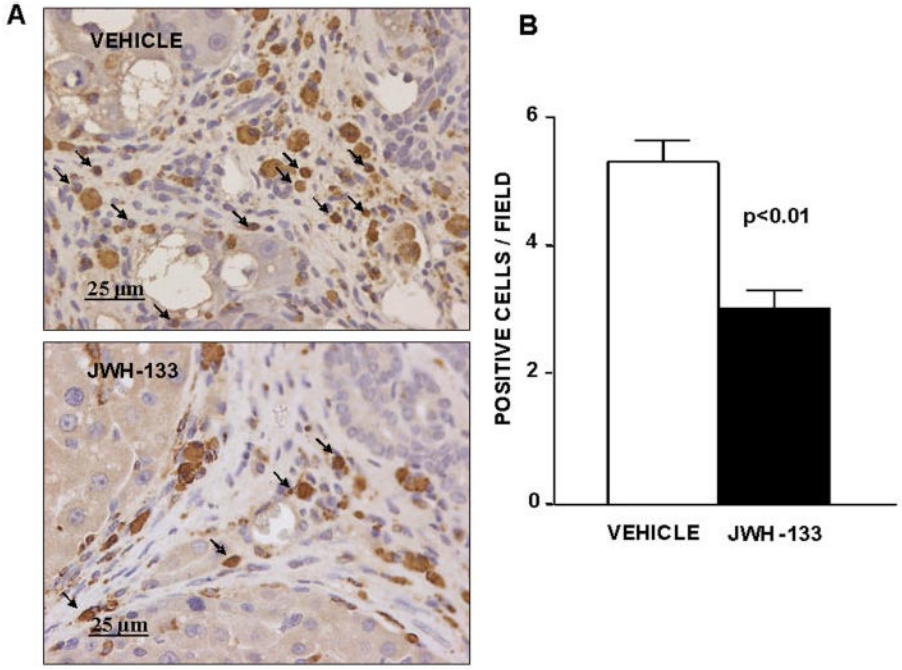

Fig. 3.

Effect of CB2 receptor activation on infiltrating cells. A, CD68 staining of a representative liver section obtained from a cirrhotic rat with ascites treated with vehicle or receiving JWH-133 (1 mg/kg b.wt. for 9 days). Positive cells were determined by counting the number of CD68-positively stained cells in 16 independent fields per animal. Original magnification, 400×. B, quantitative measurement in all animals (seven nontreated and eight treated cirrhotic rats).

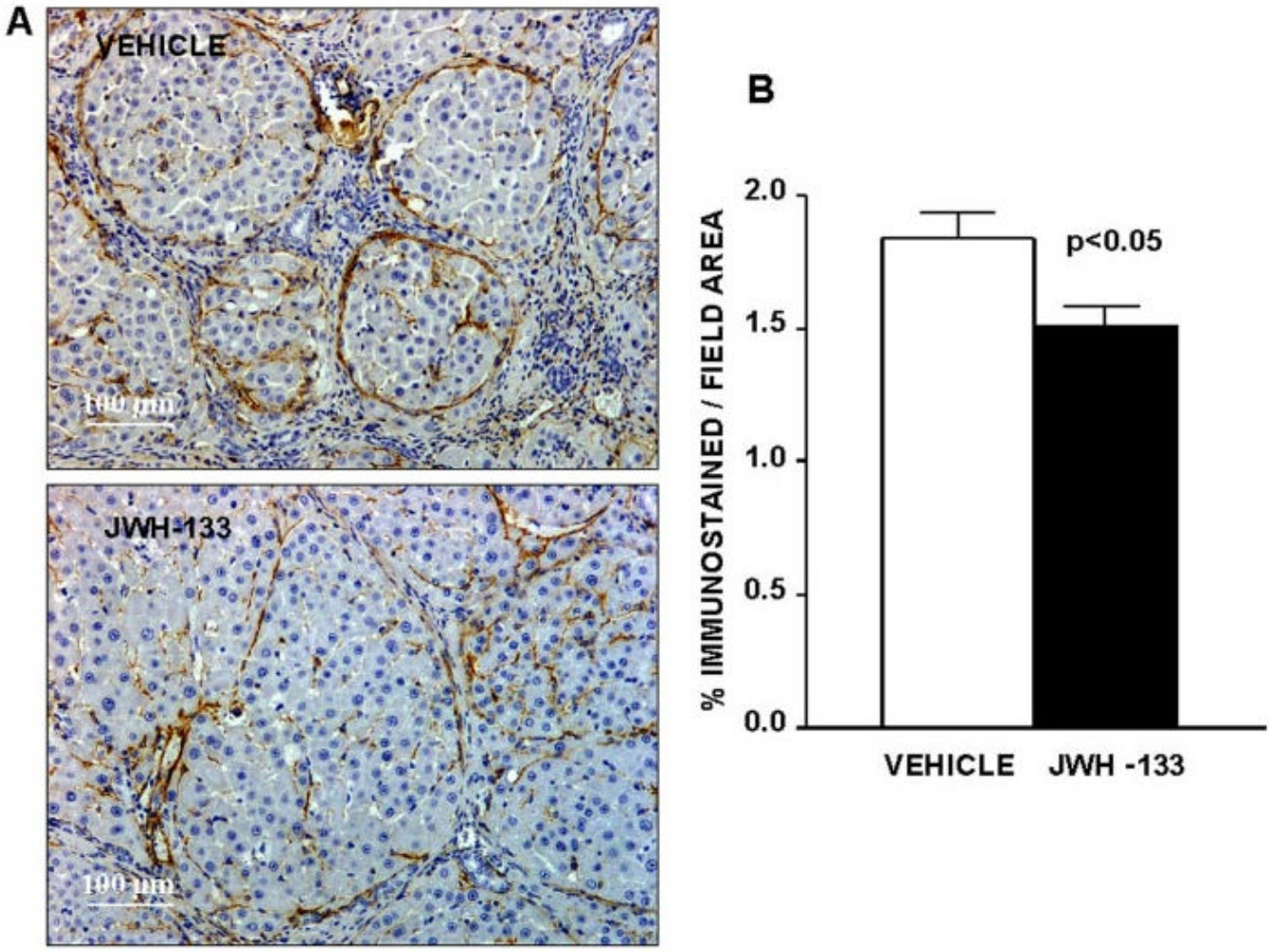

Fig. 4.

Effect of CB2 receptor activation on fibrogenic cells. A, α-SMA staining in hepatic tissue of cirrhotic rats with ascites treated with vehicle or receiving JWH-133 (1 mg/kg b.wt. for 9 days). Original magnification, 100×. Quantification of relative α-SMA-positive area was assessed in 16 fields per animal. B, quantitative measurement in all animals (seven nontreated and eight treated cirrhotic rats).

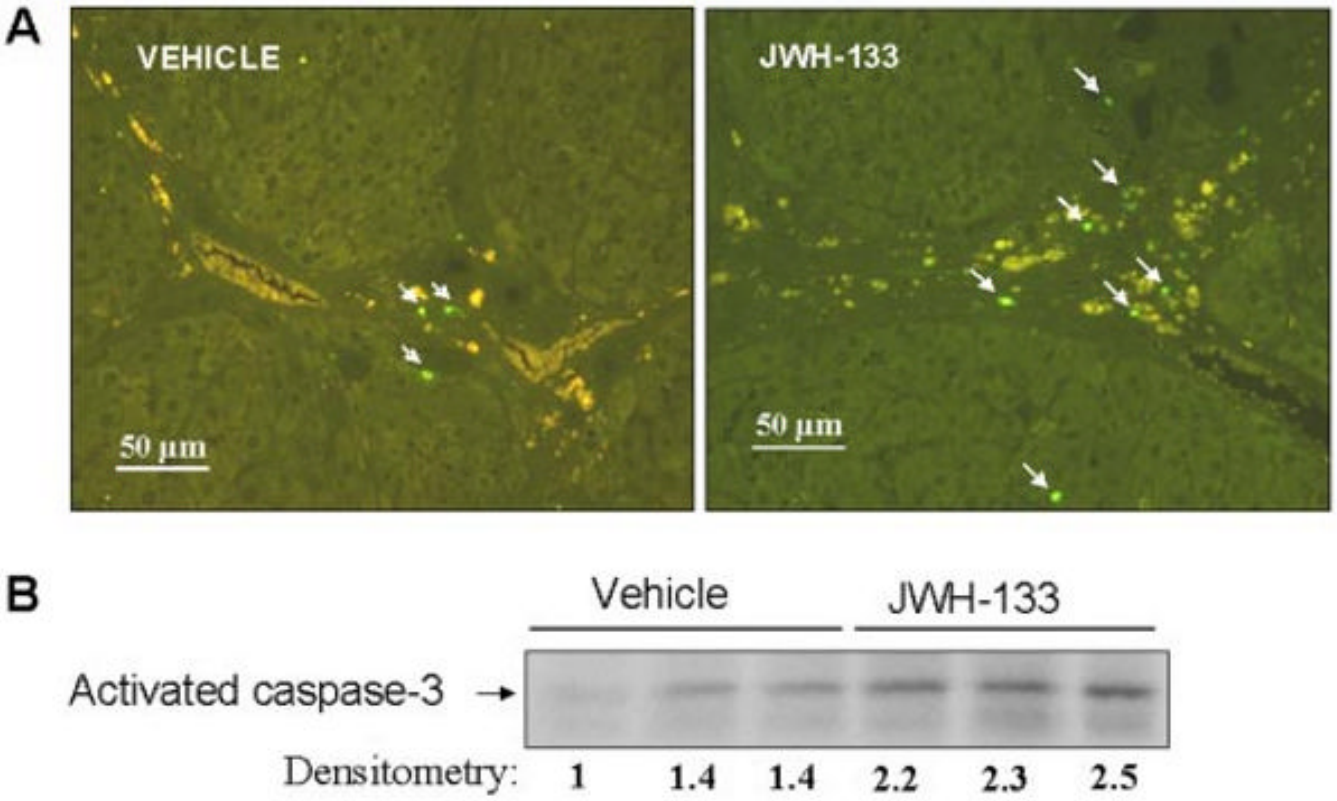

Fig. 5.

Effect of CB2 receptor activation on apoptosis. A, representative TUNEL assay in hepatic tissue of cirrhotic rats with ascites treated with vehicle or receiving JWH-133 (1 mg/kg b.wt. for 9 days). The number of positive cells was determined by counting the number of positively stained cells in eight independent fields per animal (original magnification, 200×). B, Western blot for activate caspase-3 in liver tissue of cirrhotic rats treated with vehicle or JWH-133 (1 mg/kg b.wt. for 9 days). Eighty micrograms of protein extracts was loaded per lane. Numbers below the panels indicate relative levels based on densitometry.

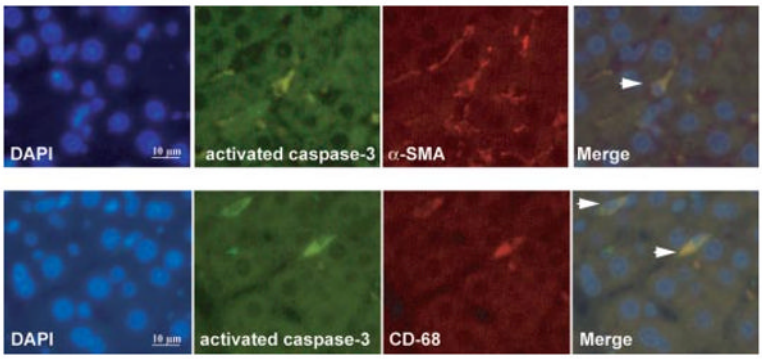

Fig. 6.

Immunofluorescent localization of activated caspase-3, α-SMA, and CD68 in livers of cirrhotic rats treated with JWH-133. Cell nuclei (blue), activated caspase-3 (green), α-SMA (red), and CD68 (red) fluorescent staining in cirrhotic livers treated with JWH-133 (1 mg/kg b.wt. for 9 days) was performed using 4,6-diamidino-2-phenylindole staining (DAPI) and specific antibodies. Colocalizations of activated caspase-3 with α-SMA (top) or CD68 (bottom) markers are shown in the merge panels (yellow; arrowheads) (n = 3). Original magnification, 400×.

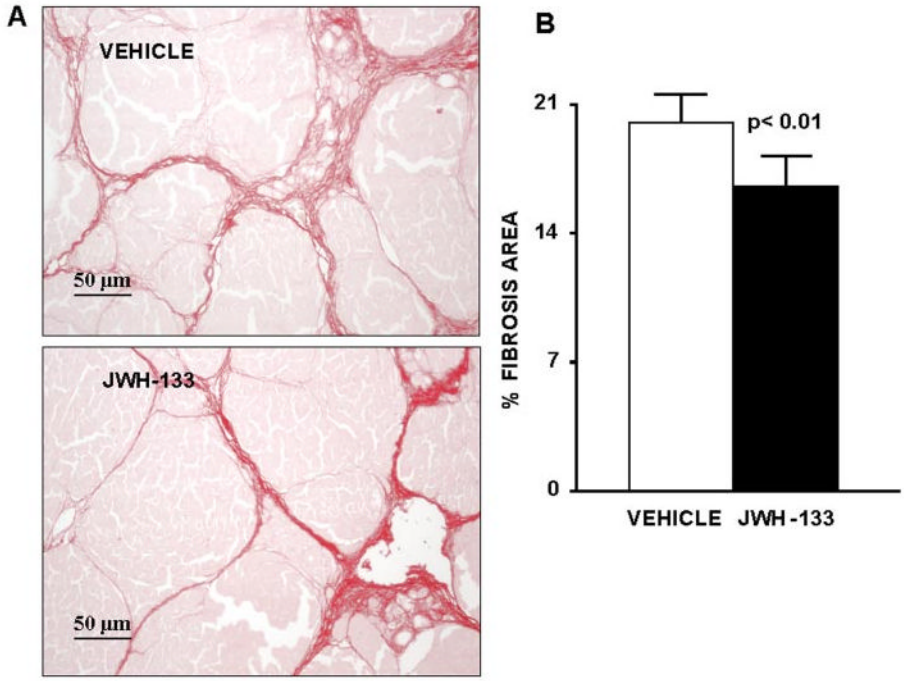

Fig. 7.

Effect of CB2 receptor activation on liver fibrosis. A, Sirius Red staining of a representative liver section obtained from a cirrhotic rats with ascites treated with vehicle ($n = 7$) or receiving JWH-133 (1 mg/kg b.wt. for 9 days; $n = 8$). Original magnification, 200×. B, quantification of relative fibrosis area was assessed in 36 fields per animal.

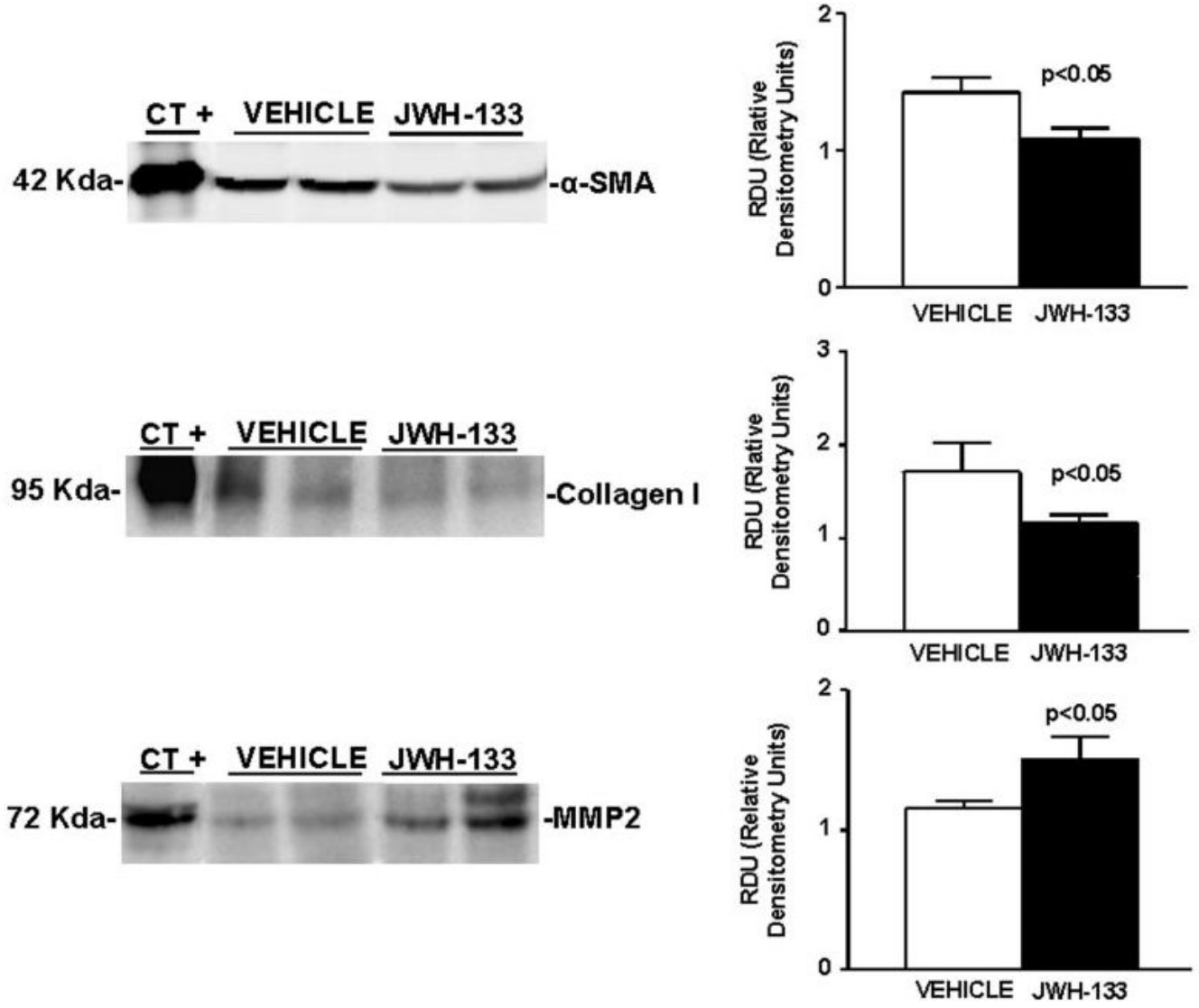

Fig. 8.

Effect of CB2 receptor activation on protein expression of α-SMA, collagen I, and MMP-2. Left, representative Western blot for α-SMA, collagen I, and MMP-2 in the liver tissue of cirrhotic rats with ascites receiving vehicle or chronically treated with JWH-133 (1 mg/kg b.wt. for 9 days). Protein extract (120, 120, and 80 μg) was loaded per lane, respectively. Protein extracts from rat thoracic aorta, skin, and thoracic aorta were used as positive control for α-SMA, collagen I, and MMP-2, respectively. Right, densitometric analysis of all samples (seven nontreated and eight treated cirrhotic rats).

TABLE 1

Standard liver function tests and serum electrolytes in cirrhotic rats with ascites receiving vehicle or the CB2 receptor agonist JWH-133 for 9 days

	Vehicle (*n* = 7)	**JWH-133 (*n* = 8)**
		1 mg · kg^{-1} · day^{-1}
Body wt (g)	482 ± 3	459 ± 15
Alanine aminotransferase (U/l)	53.6 ± 8.7	89.0 ± 10.0
Lactate dehydrogenase (U/l)	620 ± 81	578 ± 98
Total bilirubin (mg/dl)	1.10 ± 0.26	1.10 ± 0.60
Albumin (g/l)	23.2 ± 1.3	26.3 ± 0.9
Serum sodium (mEq/l)	144 ± 1	143 ± 2
Serum potassium (mEq/l)	4.7 ± 0.4	4.0 ± 0.5
Serum osmolality (mOsm/kg)	293 ± 3	299 ± 3